

L.I.Anatychuk^{1,2}, A.V.Prybyla¹



L.I. Anatychuk

¹Institute of Thermoelectricity of the
NAS and MES of Ukraine, 1, Nauky str.,
Chernivtsi, 58029, Ukraine

²Yu. Fedkovych Chernivtsi National University, 2,
Kotsyubinsky str., Chernivtsi, 58000, Ukraine



A.V. Prybyla

OPTIMIZATION OF POWER SUPPLY SYSTEM OF THERMOELECTRIC LIQUID-LIQUID HEAT PUMP

The paper presents the results of computer simulation of liquid-liquid thermoelectric heat pump. The most rational variants of power supply to heat pump have been considered. Multi-parameter computer optimization has been used to determine parameters of power supply system of thermoelectric heat pump making possible to increase its heating coefficient by 15%.

Key words: thermoelectric heat pump, computer simulation, water recovery system.

Introduction

General characterization of the problem. The use of thermoelectric heat pumps (THP) in air and liquid conditioning systems, special-purpose evaporators is related to their unique properties [1 – 5].

An example of efficient application of thermoelectric heat pumps is provided by systems of water recovery from liquid biowaste on board of manned spacecrafts (urine, atmosphere humidity condensate, sanitary-hygiene water) [4, 5].

Paper [8] presents the results of computer simulation of liquid-liquid thermoelectric heat pump. Multi - parameter computer optimization has been used to determine design parameters of the arrangement of thermoelectric modules and heat exchangers of thermoelectric heat pump. The next step of this work is computer optimization of the parameters of power supply system of thermoelectric heat pump, making possible its further efficiency increase.

The purpose of this work is to increase the efficiency of power supply system of thermoelectric heat pump by means of multiparameter computer simulation and optimization.

Physical model of THP

A physical model of thermoelectric heat pump is represented in Fig. 1. It comprises a liquid heat exchange system assuring passage of heat flux Q_c through the cold side of thermoelectric modules 1, thermoelectric modules 2 consisting of semiconductor n - and p - type legs and a liquid heat exchange system 3 assuring passage of heat flux Q_h through their hot side.

Heat carrier (urine, atmospheric humidity condensate, sanitary-hygiene water) circulates in liquid heat exchange system at a rate of G ml/s. Two variants of heat carrier connection were considered. In the first case heat carriers in the hot 3 and cold 1 heat exchange system move in the same direction (1.1 → 1.2; 2.1 → 2.2), and in the second case – opposite to each other (1.1 → 1.2; 2.2 → 2.1).

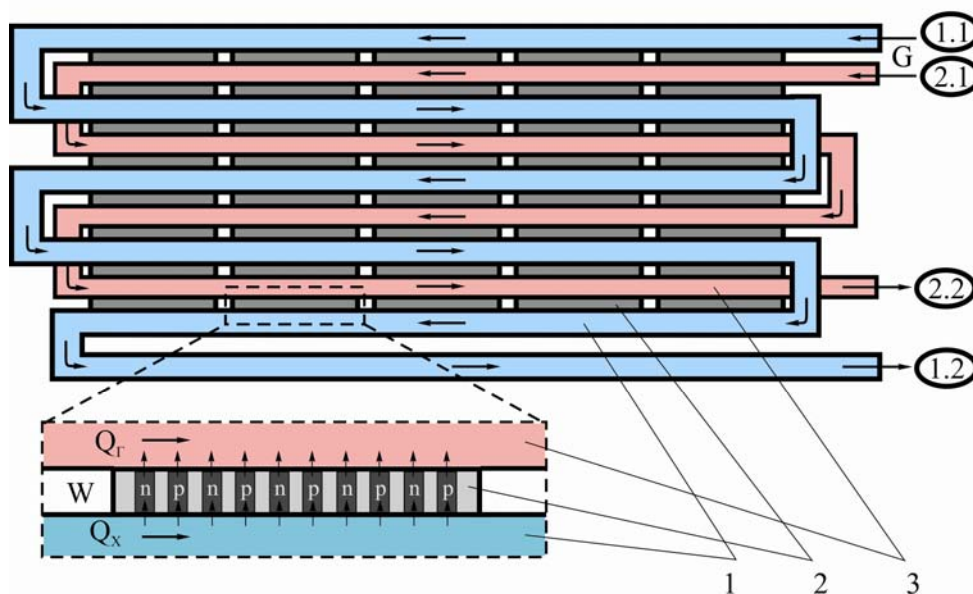


Fig. 1. Physical model of thermoelectric heat pump.

Moreover, various variants of power supply W to thermoelectric modules 2 were considered:

- 1) all the modules are powered by the same current and voltage, optimal for the entire heat pump;
- 2) the modules are grouped into sections with individually optimized power supply;
- 3) power supply to all thermoelectric modules is done individually.

Mathematical and computer description of the model

To describe heat and current fluxes, let us use the laws of conservation of energy

$$\operatorname{div} \vec{E} = 0 \tag{1}$$

and electric charge

$$\operatorname{div} \vec{j} = 0, \tag{2}$$

where

$$\vec{E} = \vec{q} + U\vec{j}, \tag{3}$$

$$\vec{q} = \kappa \nabla T + \alpha T \vec{j}, \tag{4}$$

$$\vec{j} = -\sigma \nabla U - \sigma \alpha \nabla T. \tag{5}$$

Here \vec{E} is energy flux density, \vec{q} is thermal flux density, \vec{j} is electric current density, U is electric potential, T is temperature, α , σ , κ are the Seebeck coefficient, electric conductivity and thermal conductivity.

With regard to (3) – (5), one can obtain

$$\vec{E} = -(\kappa + \alpha^2 \sigma T + \alpha U \sigma) \nabla T - (\alpha \sigma T + U \sigma) \nabla U. \tag{6}$$

Then the laws of conservation (1), (2) will acquire the form:

$$-\nabla \left[(\kappa + \alpha^2 \sigma T + \alpha U \sigma) \nabla T \right] - \nabla \left[(\alpha \sigma T + U \sigma) \nabla U \right] = 0, \tag{7}$$

$$-\nabla (\sigma \alpha \nabla T) - \nabla (\sigma \nabla U) = 0. \tag{8}$$

These nonlinear differential equations of second order in partial derivatives (7) and (8) determine the distribution of temperature T and potential U in thermoelements.

An equation describing the process of heat transport in the walls of heat exchangers in the

steady-state case is written as follows:

$$\nabla(-k_1 \cdot \nabla T_1) = Q_1, \quad (9)$$

where k_1 is thermal conductivity of heat exchanger walls, ∇T_1 is temperature gradient, Q_1 is heat flux.

The processes of heat-and-mass transfer in heat exchanger channels in the steady-state case are described by equations [9]

$$-\Delta p - f_D \frac{\rho}{2d_h} v |\vec{v}| + \vec{F} = 0, \quad (10)$$

$$\nabla(A\rho\vec{v}) = 0, \quad (11)$$

$$\rho A C_p \vec{v} \cdot \nabla T_2 = \nabla \cdot A k_2 \nabla T_2 + f_D \frac{\rho A}{d_h} |\vec{v}|^3 + Q_2 + Q_{wall}, \quad (12)$$

where p is pressure, ρ is heat carrier density, A is cross-section of the tube, \vec{F} is the sum of all forces, C_p is heat carrier heat capacity, T_2 is temperature, \vec{v} is velocity vector, k_2 is heat carrier thermal conductivity, f_D is the Darcy coefficient, $d = \frac{4A}{Z}$ is effective diameter, Z is perimeter of tube wall, Q_2 is heat which is released due to viscous friction [W/m] (from the unit length of heat exchanger), Q_{wall} is heat flux coming from the heat carrier to tube walls [W/m]

$$Q_{wall} = h \cdot Z \cdot (T_1 - T_2), \quad (13)$$

where h is heat exchange coefficient which is found from equation

$$h = \frac{Nu \cdot k_2}{d}. \quad (14)$$

The Nusselt number is determined with the use of the Gnielinski equation ($3000 < Re < 6 \cdot 10^6$, $0.5 < Pr < 2000$)

$$Nu = \frac{\left(\frac{f_d}{8}\right)(Re - 1000)Pr}{1 + 12.7\left(\frac{f_d}{8}\right)^{\frac{1}{2}}\left(Pr^{\frac{2}{3}} - 1\right)}, \quad (15)$$

where $Pr = \frac{C_p \mu}{k_2}$ is the Prandtl number, μ is dynamic viscosity, $Re = \frac{\rho v d}{\mu}$ is the Reynolds number.

To determine the Darcy coefficient f_D we will use the Churchill equation for the entire spectrum of the Reynolds number and all values of e/d (e is roughness of wall surface)

$$f_D = 8 \left[\frac{8}{Re}^{12} + (A + B)^{-1.5} \right]^{1/12}, \quad (16)$$

where $A = \left[-2.457 \cdot \ln \left(\left(\frac{7}{Re} \right)^{0.9} + 0.27(e/d) \right) \right]^{16}$, $B = \left(\frac{37530}{Re} \right)^{16}$.

Solving Eqs.(7) – (12), we obtain the distributions of temperatures, electric potential (for thermoelements), velocities and pressure (for heat carrier).

The above differential equations with the respective boundary conditions were solved using Comsol Multiphysics package of applied programs. It was used to perform a multiparameter

optimization of thermoelectric heat pump design and to determine the electric and thermal parameters for the achievement of boundary values of its heating coefficient when assuring the possibility of THP operation under severe conditions of manned space missions.

Computer simulation results

The external appearance of thermoelectric heat pump is represented in Fig. 2.

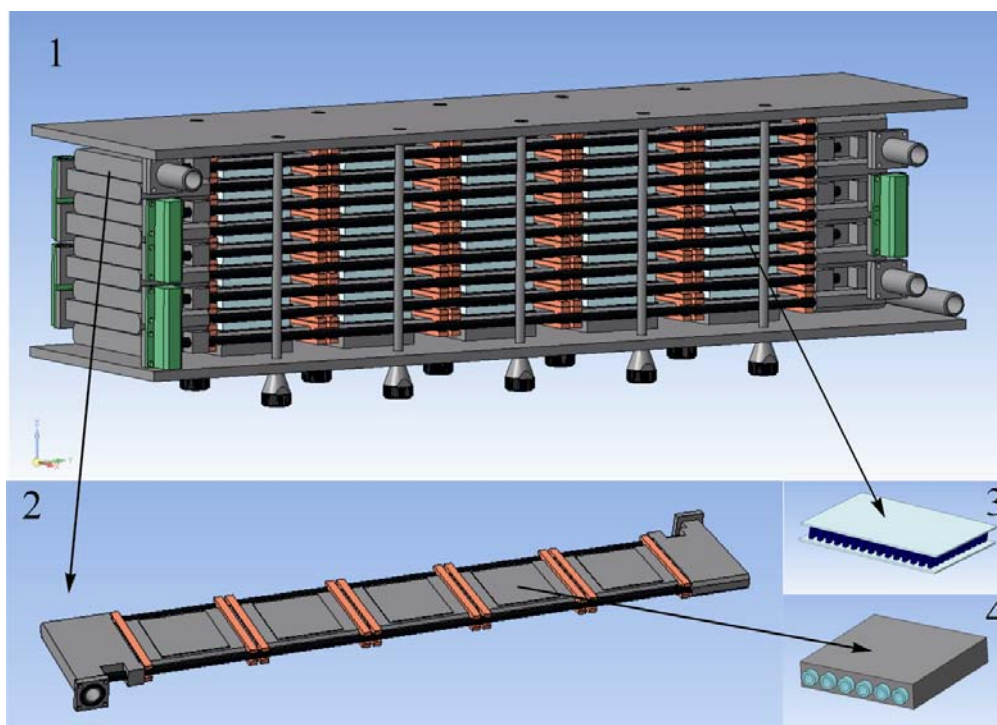


*Fig. 2. Thermoelectric heat pump:
1 – external appearance, 2 – schematic of connection of
one row of heat exchangers 4, 3 – thermoelectric modules.*

Below are given the results of optimization of the parameters of electric power supply to thermoelectric modules (according to model in item 1) for real thermal and temperature operating conditions of the heat pump. The results of computer investigations of thermoelectric module design, as well as heat exchange system are very important and will be presented in detail in the next work.

The initial data:

- electric power supply to thermoelectric modules – 300 W;
- the number of thermoelectric modules – 80 pcs;
- heat carrier temperature at inlet to hot heat transfer loop – 36°C;
- heat carrier temperature at inlet to cold heat transfer loop – 31.5°C;
- hydraulic resistance of each heat-transfer loop – not more than 0.07 atm;
- heat carrier flow rate in each loop – not more than 22 ml/s.

Thus, the values of integral heating coefficient were calculated for different variants of electric power supply to thermoelectric modules:

- 1) all the modules are powered by the same current and voltage, optimal for the entire heat pump;
- 2) the modules are grouped into two sections with individually optimized power supply;
- 3) the modules are grouped into four sections with individually optimized power supply;
- 4) all thermoelectric modules are powered by optimal current individually (80 conventional sections).

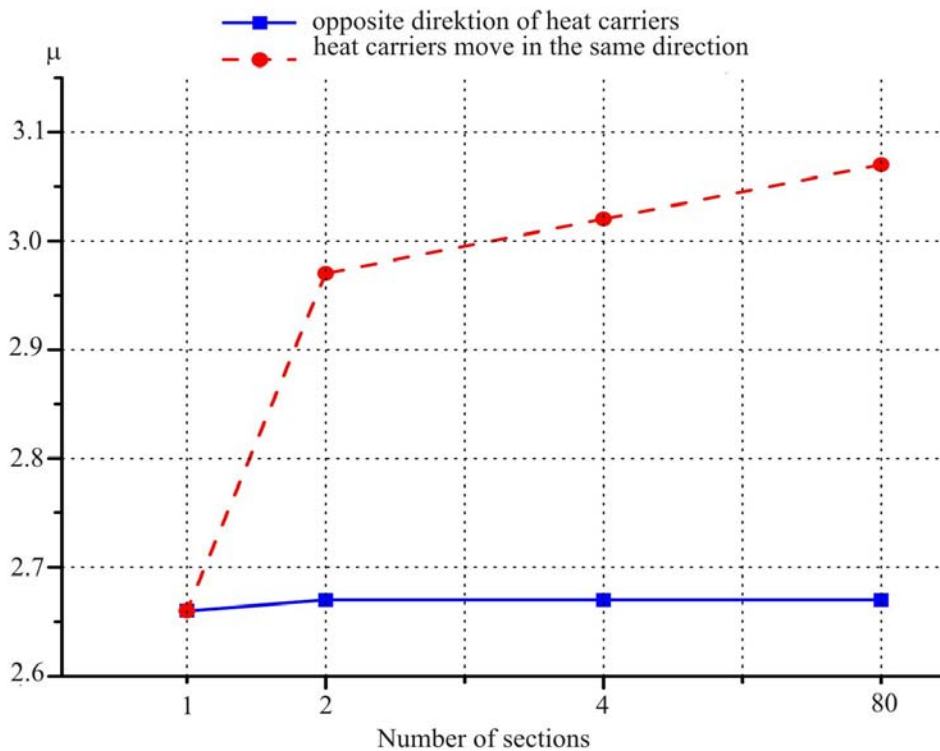


Fig. 3. Heating coefficient of thermoelectric heat pump versus the number of sections for two different hydraulic connections of heat carriers.

According to the results of simulation (Fig. 3), with such a hydraulic connection of the hot and cold heat exchange loops, when both heat carriers move in the opposite directions (direction 1.1 → 1.2; 2.2 → 2.1 in Fig. 1), the heating coefficient of the heat pump is essentially independent of the number of sections and is at the level of $\sim 2.6 \div 2.7$. However, in the case when heat carriers move in the same direction (direction 1.1 → 1.2; 2.1 → 2.2 in Fig. 1), increasing the number of sections with individual optimal power supply leads to heating coefficient growth to $\sim 3.0 \div 3.1$. The increase in heating coefficient of thermoelectric heat pump by 15% for such conditions is due to the fact that dependence of heating coefficient of thermoelectric modules on temperature difference and supply current in each section is nonlinear. In this case the use of several independent sections allows most efficient realization of all the advantages of thermoelectric power conversion in each temperature range.

Conclusions

1. The method of multiparameter computer optimization of thermoelectric heat pumps has been developed.
2. The optimal energy parameters of thermoelectric heat pump have been calculated for real conditions of its operation.
3. It has been established that increasing the number of sections of thermoelectric heat pump with individual electric power supply to each section results in the growth of integral heating coefficient by 15%.
4. It has been shown that the most efficient hydraulic connection of the hot and cold heat exchange loops is the case when both heat carriers move in the same direction.

References

1. Yu.Yu.Rozver, Thermoelectric Air-Conditioner for Vehicles, *J.Thermoelectricity* 2, 52 – 56 (2003).
2. L.I.Anatychuk, L.M.Vikhor, and Yu.Yu.Rozver, Investigation on Performance of Thermoelectric Cooler of Liquid or Gas Flows, *J.Thermoelectricity* 1, 73 – 80 (2004).
3. L.I.Anatychuk, N.Suzuki, and Yu.Yu.Rozver, Indoor Thermoelectric Air-Conditioner, *J.Thermoelectricity* 3, 53 – 56 (2005).
4. V.G.Rifert, V.I.Usenko, P.A.Barabash at al., Development and Test of Water Regeneration System from Liquid Biowaste on Board of Manned Spacecrafts with the Use of Thermoelectric Heat Pump *J.Thermoelectricity* 2, 63 – 74 (2011).
5. L.I.Anatychuk, P.A.Barabash, V.G.Rifert, Yu.Yu.Rozver, V.I.Usenko, and R.G.Cherkez, Thermoelectric Heat Pump as a Means of Improving Efficiency of Water Purification Systems for Biological Needs on Space Missions, *J.Thermoelectricity* 6, 78 – 83 (2013).
6. L.I.Anatychuk, Rational Areas of Thermoelectric Research and Applications, *J.Thermoelectricity* 1, 3 – 14 (2001).
7. L.I. Anatychuk, Current Status and Some Prospects of Thermoelectricity, *J.Thermoelectricity* №2, 7 – 20 (2007).
8. L.I.Anatychuk, A.V.Prybyla, On the Effect of Arrangement of Thermoelectric Modules and Heat Exchangers on the Efficiency of Liquid-Liquid Heat Pump, *J.Thermoelectricity* №4, p. 44 – 49 (2015).

Submitted 10.12.2015